SciMedCentral

Journal of Autoimmunity & Research

Case Report

Gene Expression and Pathway Analysis of Radiation-Induced Apoptosis in C-4 I Cervical Cancer Cells

Walid Mahmoud Khalilia[1]*, Gül Özcan[2], and Songül Karaçam[3]

[1]*Institute of Science, Istanbul University, Turkey*
[2]*Department of Science, Istanbul University,Turkey*
[3]*Department of Radiation Oncology, Istanbul University, Turkey*

***Corresponding author**
Walid Mahmoud Khalilia, Institute of Science, Department of Radio biology, Istanbul University, A-Blok, 34134, Vezneciler-Fatih, Istanbul – Turkey, Tel: 95334957323; Fax: 90-212 5280527; Email: khaliliawalid@gmail.com

Submitted: 23 November 2016

Accepted: 14 February 2017

Published: 21 February 2017

Keywords
- Apoptosis
- C-4 I cells
- Gamma radiation
- Microarray
- qRT-PCR

Abstract

Objective: The present study aimed to determine whether a single-fraction of gamma radiation could induce the expression of specific genes involved in apoptosis signaling pathways, which helps us in better understanding cancer dynamics and treatment targets for cancer.

Materials and methods: C-4 I cells were treated with a single fraction of gamma radiation at various doses (0, 2, 8, 16, 32 and 64 Gy) and investigated after incubation for five time periods (0, 24, 48, 60 and 72 h). The proliferation of C-4 I cells was measured by MTT assay, but apoptotic index (AI) and apoptotic morphological features were assessed by fluorescent microscopy. Moreover, the expression of the apoptotic genes was evaluated using microarray and qRT-PCR molecular processes. In addition, gene ontology and pathway analysis were performed.

Results: Gamma irradiation inhibits proliferation of C-4 I cells in a dose- and time-dependent manner, and 16 Gy was identified as the IC50 and AI dose. Microarray and qRT-PCR results monitored the expression of some factors that are known apoptosis activators were up regulated by gamma radiation treatment, whereas some anti-apoptosis members were down regulated.

Pathway analysis identified that significant pathways related to apoptosis, cell cycle and P53 were significantly enriched.

Conclusions: These results provide evidence that gamma radiation directly induces anti-proliferative effects by altering the expression of genes associated with cell proliferation and apoptosis pathways in C-4 I cells.

ABBREVIATIONS

IR: Ionizing Radiation; TNF: Tumor Necrosis Factor; MTT: 3-[4, 5-Dimethylthiazol-2-yl]-2, 5-Diphenyltetrazolium bromide; DAPI: 4,6-Diamidino-2-phenylindole; AI: Apoptotic Index; FC: Fold Change; GO: Gene Ontology; mCt: Mean threshold cycle.

INTRODUCTION

Radiation therapy is one of the most common treatments for cancer, used in more than half of all cancer cases, in which high-energy rays used to destroy cancer cells in the body. Radiotherapy is the most effective therapy for cervical cancer in advanced stages [1]. Ionizing radiation (IR) leads to many cellular changes like activates signaling pathways in the nucleus as a result of DNA damage, and signaling pathways initiated at the level of the plasma membrane. DNA damage result in a coordinate network of signal transduction pathways involved in cell cycle arrest, apoptosis, stress response and the activation of DNA repair processes. However, the plasma membrane signaling pathways through activation of some receptors results in activation of the initiator caspase-8 which can propagate the apoptosis signal by direct cleavage of downstream effectors caspases. IR can also induce apoptosis via the generation of free radical oxygen species, which gives rise to a variety of cellular lesions including both DNA and membrane damage [2]. Previous studies suggest that changes in membrane fluidity, superoxide dismutase (SOD) and calcium level were involved in the mechanism of radiation induced cervical cells apoptosis. Moreover, apoptotic sensitivity of these cells after the first dose of radiation treatment showed

a direct correlation with the radiation treatment outcome in patients after completion of radiotherapy protocol (70 Gy) [3].

Apoptosis is the major mode of programmed cell death, and is characterized by a series of morphological hallmarks, including cell shrinkage, nuclear DNA condensation and fragmentation, as well as plasma membrane blebbing, which formed the apoptotic bodies. There are two main apoptotic pathways: the extrinsic initiated by death receptors and the intrinsic pathway initiated by mitochondrial events. However, there is evidence that the two pathways are linked and that molecules in one pathway can affect the other. Although, there is an additional apoptotic pathway under studies yet [4].

Apoptosis is a genetically regulated biological process. Changes on apoptotic cells occur after a series of events regulated by caspases and various cell signals that regulate pro-apoptotic and anti-apoptotic proteins. Extrinsic and intrinsic pathways can be activated separately, but most caspases activation is common in an apoptotic pathway. Ligand-bound tumor necrosis factor (TNF) receptors initiate apoptosis by recruiting fas associated death domain (FADD) and other death domain adaptor proteins that then recruit and activate caspases [5,6]. Environmental stresses trigger BCL2 protein oligomerization and insertion into the mitochondrial membrane [7,8], releasing apoptotic protease activating factor 1 (APAF1) and other caspase activation and recruitment domain (CARD) family members that also oligomerize to recruit and activate caspases [4,9,10]. Caspases promote a proteolysis cascade that degrades cellular protein targets, while the inhibitor of apoptosis protein (IAP) family directly inhibits caspases. One of the major apoptosis signaling pathways involves the P53 tumor suppressor. Tumor protein P53 is a nuclear transcription factor that regulates the expression of a wide variety of genes involved in apoptosis in response to genotoxic or cellular stress [2,11]. Understanding apoptosis is often considered a key to understanding the genesis of tumors and to devising innovative strategies for cancer treatment [12].

Therefore, the present study aimed to determine whether gamma radiation could induce the expression of specific genes involved in apoptosis signaling pathways. Identifying up-regulated or down-regulated genes helps us in better understanding the cancer dynamics and helps identify markers and treatment targets for cervical cancer.

MATERIALS AND METHODS

Cell culture and γ^{-60}co irradiation

Cervical cancer C-4 I cell line (ATCC), maintained at 37°C in Waymouth's MB 752/1 (Sigma) supplemented with 10% fetal bovine serum (Gibco Lab.), 100 IU/ml penicillin (Pronapen, Pfizer) and 100 go/ml streptomycin (streptomycin sulfate, İ.E. Ulagay) in a humidified atmosphere of 5% CO_2. Cells were "passaged" every 2 to 3 days using 0.25% trypsin (Sigma) to detach the cells from the flasks [13]. Before the cell proliferation and apoptosis assays, and prior to evaluating genes expression, C-4 I cells were placed in a 6-well plate at a density of 2.5×10^5 cells per well. After overnight incubation, cells were irradiated at the Istanbul University, Faculty of Medicine, Radiation Oncology, Turkey (Cirus, CCR CisBio, Canada) by different dozes of gamma radiation (2, 8, 16, 32 and 64 Gy) with a dose rate of 100 cGy/min. and incubated for 24, 48, 60 and 72 h, control group (0 Gy) were not irradiated. After irradiation, cell cultures were replaced in the incubator and maintained at 37°C under 5% CO_2. For the irradiation groups, the time when the irradiation was finished was set as time 0 [14,15].

Cytotoxicity and cell proliferation

Cell proliferation was evaluated using the 3-[4, 5-Dimethylthiazol-2-yl]-2, 5-Diphenyltetrazolium bromide (MTT; Sigma) cell viability assay, as previously described [16].

Observation of morphological changes

The cellular morphological changes were observed using phase contrast microscopy and fluorescent microscopy [13].

Apoptotic index (AI)

After irradiation and incubation, C-4 I cells were trypsinized, washed with mixture of 200 µl methanol: farnesyl thiosalicylic acid (FTS) (1:1), fixed in iced pure methanol, stained with 50µg/mL of 4,6-diamidino-2-phenylindole (DAPI, Sigma) in dark for 20 minutes, and then the slides were washed in phosphate buffered saline (PBS). DAPI is a blue-fluorescent DNA stain that exhibits ~20-fold enhancement of fluorescence upon binding to AT regions of dsDNA. It is commonly used as a nuclear counter stain in fluorescence microscopy. Because of its high affinity for DNA, it is also frequently used for counting cells, measuring apoptosis, sorting cells based on DNA content.

The nuclear morphology was observed under a fluorescent microscope (λex. 358 nm, λem. 461 nm). And apoptotic cells were identified by their characteristic fragmented chromatin masses. Small groups of apoptotic bodies were counted as remnants of one apoptotic cell. Apoptotic cells were counted among 100 cells randomly. Apoptosis was expressed as the number of apoptotic nuclei per number of total nuclei counted in the same microscopic field. This AI was a mean of three independent experiments [12,16].

Isolation and quantification of total RNA

C-4 I cells were plated in a 6-well plate at a density of 2.5×10^5 cells per well. After overnight incubation cells were irradiated by 16 Gy single dose of $\gamma^{-60}Co$ radiation and incubated for 60 hours, control group (0 Gy) were not irradiated. After wash with PBS, $6x10^6$ cells were harvested from samples and total RNA was extracted using High Pure RNA Isolation kit (Roche) according to the manufacturer's instructions. RNA concentrations were determined with visible spectrophotometer (GBC Cintra 20). RNA purity was checked by measurement of the A 260/280 nm ratio, which was routinely in the range of 1.8-2.0. Purified total RNA samples were stored frozen at -80°C until needed for subsequent gene expression profiling [17].

Bead array technology

Human HT-12 Expression Bead Chips with the Illumina Whole-Genome Gene Expression Direct Hybridization Assay (Illumina) system were used to evaluate the expression patterns of more than 48,000 transcripts in C-4 I cells, according to the manufacturer's instructions. Complementary DNA (cDNA) was produced following reverse transcription from 100 ng of total

RNA and then fluorescent cRNA was performed according to the TargetAmp™-Nano Labeling Kit (Illumina). 750 ng cRNA per sample, which was then hybridized to Human HT-12 Illumina® Expression BeadChip® (Illumina) [18].

Bead Chip scanning and data analysis

Microarray slides were then scanned using the Illumina iScan System (Illumina). For gene expression analysis and the generation of gene lists for fold change (FC), functional annotation and pathway analysis, microarray data were processed in a Genome Studio module (V2011.1; Illumina). The signal was taken as the measure of mRNA abundance derived from the level of gene expression. Raw data were adjusted by using Box Plots normalization. Significance levels of differences between the groups were calculated for each probe set using FC and P-values ($p < 0.05$ and $FC \geq |2|$) [19,20].

Bioinformatics analysis

Differentially expressed genes were used as input for a network analyses that were performed with Gene Ontology (GO) network building tools (PANTHER, http://www.pantherdb.org/pathway/). GO and pathway analysis were performed on the up-regulated and down-regulated genes. Significant functions were identified based on p-value ($p < 0.05$) [21].

qRT-PCR technology

A Real Time Ready Apoptosis Panel (Human Apoptosis Panel, 96, Roche) was used to assess expression patterns of apoptosis-related genes in C-4 I cells, according to the manufacturer's instructions. The panel is designed for expression profiling of genes that play a major role in apoptotic processes in human cells. On the plate, assays for the 84 apoptosis-related genes are grouped to reflect the various protein families and pathways involved in apoptosis.

cDNA synthesis and qRT-PCR set up

First-strand cDNA was synthesized from 3 µg total RNA and a primer was performed using the cDNA synthesis kit (Transcriptor High Fidelity cDNA Synthesis kit, Roche) following manufacturer instructions [22].

Eighty-four apoptosis-related genes were quantified using a Real Time Ready Apoptosis Panel (Human Apoptosis Panel, 96, Roche) according to manufacturer instructions. PCR mix for one reaction (20 µl) that was done by adding 2 µl of primer-probe mix and 10 µl probe and 3 µl dH2O to a total volume of 15 µl in a 1.5 ml reaction tube on ice. After mixing carefully, the 15µl mixture was pipetted into each well of the 96 well plate (Light Cycler 480® Multiwell plate, Roche). After that a 5 µl cDNA template was added to each well, and the plate was sealed with sealing foil and centrifuged for 2 minutes at 1500 *xg* followed by loading the multi well plate into the instrument (Light Cycler 480® Instrument II, Roche). All reactions were run for one cycle of PCR that consisted of enzyme activation and template denaturation for 10 minutes at 95°C, followed by 40 cycles of PCR. Each cycle consisted of 30 second annealing at 60°C and an extension phase at 72°C for 1 second followed by 20 seconds at 85°C to denature the double-helix PCR product. Fluorescence data was acquired after each annealing and extension step. Results were expressed using the comparative threshold (Ct) method [23].

Quantitative data analysis of qRT-PCR

Calculation of gene expression was carried out using Ct cycle. The mean threshold cycle (mCt) was obtained from triplicate amplifications during the exponential phase. The mCt value of reference genes was then subtracted from mCt value of the target genes to obtain the ΔCt and ΔΔCt values of each sample, which were calculated from corresponding Ct values; where ΔΔCt= [mCt target – mCt reference] (treated sample) - [mCt target – mCt reference] (untreated sample). Finally, a target gene expression/reference gene expression ratio was calculated using the ratio formula (ratio = $2^{-\Delta\Delta Ct}$), which was used for gene expression analysis and the generation of gene lists for FC ($FC \geq |2|$) [24].

Statistical analysis

For the experimental cell proliferation and AI data sets, statistical significance was determined using one-way ANOVA and unpaired Students't test ($p < 0.05$).

RESULTS AND DISCUSSION

Initial studies on the treatment of a cervical cancer adenocarcinoma C-4 I cells with 2, 8, 16, 32 and 64 Gy of $\gamma^{-60}Co$ radiation for a duration of 0-72 hours indicated tha tradiation inhibits C-4 I cells proliferation and apoptosis was elevated by time and $\gamma^{-60}Co$ radiation dose rate, with maximum levels observed 60 hours after irradiation.

Cell proliferation

MTT assay showed that radiation inhibited proliferation of C-4 I cells. Our results showed that C-4 I cell survival rates of all irradiated groups at 0-hour post-irradiation time were nearly the same at more than 70%, while the cell survival at 24 hours post-irradiation time in the 16, 32 and 64 Gy groups were much lower, less than 70%. Our experiments showed that a radiation dose of 16 Gy induced cell death in 50% of C-4 I cells at 24 hours post-irradiation time compared with control group (0 Gy). A such a 16 Gy $\gamma^{-60}Co$ radiation dose was determined as the IC_{50} dose (Figure 1).

Microscopy and apoptotic index (AI)

Fluorescent images of the nuclear morphology of C-4 I cells in control and in all irradiated groups (2, 8, 16, 32 and 64 Gy) at 60 hours post-irradiation time after DAPI staining. The nuclei were normal in the control group; whereas the nuclei became condensed or fragmented in the all irradiated groups (2, 8, 16, 32 and 64 Gy) (Figure 2).

AI was induced by $\gamma^{-60}Co$ radiation, and increased in a radiation dose and time-dependent manner (Figure 3). The highest AI values (at 60 and 72 hours post-irradiation time) were reached more than 50% for 64 Gy and 32 Gy. While, at 0 and 24 hours post-irradiation time the lowest AI values, less than 20% for all irradiated groups. Apoptosis levels remained nearly stable for durations ranging from 60 to72 hours post-irradiation time (Figure 3). 16 Gy $\gamma^{-60}Co$ radiation dose was determined to be the optimum AI value in our current study.

Gamma radiation cytotoxicity and AI considering 16 Gy as the IC_{50} and optimum AI dose, based on these data, 16 Gy group at 60-hour time point was chosen for further studies.

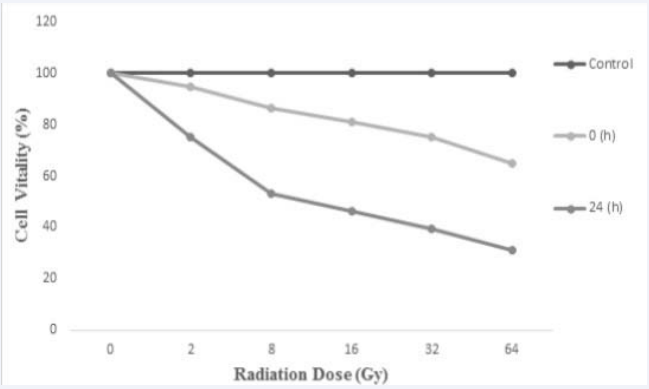

Figure 1 Effect of γ-60Co radiation on survival of C-4 I cells at 0 and 24 hours post-irradiation time. Cell survival was determined by MTT assay. Results are presented as a percent of control. Control is 100% in all time points. The experiment was repeated triple with similar results.

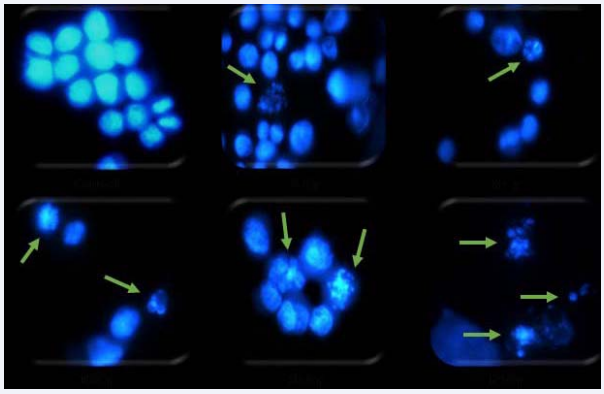

Figure 2 Representative fluorescent images of the nuclear morphology of C-4 I cells in the control and all irradiated (2, 8, 16, 32 and 64 Gy) groups at 60 hours post-irradiation time, following DAPI staining. In control group, cellular nuclear chromatin homogeneous distribution; whereas the nuclei became condensed or fragmented in the all irradiated groups observed by a fluorescence microscope (X1000). Arrows represent apoptotic cells. The experiment was repeated triple with similar results.

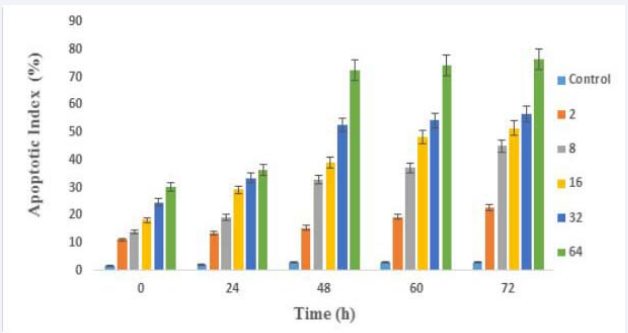

Figure 3 Measure of apoptotic index by counting 100 of C-4 I cells in the control and all irradiated (2, 8, 16, 32 and 64 Gy) groups at 24, 48, 60, and 72 hours post-irradiation time, following DAPI staining under fluorescence microscope (×1000). The data shown represents mean of three independent experiments.

In the present study, C-4 I cell growth was depressed by large doses of $\gamma^{-60}Co$ radiation (8, 16, 32 and 64 Gy), but not by low doses (2) at 24 hours post-irradiation time. These results are in agreement with those of previous studies [25]. In addition to decreasing cell proliferation and viability, a single dose of $\gamma^{-60}Co$ radiation induced apoptosis in C-4 I cells. From our results the percentage of condensed or fragmented nuclei increased with time and dose of radiation. These results are consistent with those of previous studies [26].

The percentages of apoptotic cells in AI assay was showed that the level of apoptosis increased with $\gamma^{-60}Co$ radiation dose. These results indicate that irradiation primarily affects the C-4 I cell proliferation by inducting cell apoptosis. These results are consistent with those of previous studies [12].

Gene expressions by microarray and pathway analysis

For statistical analysis of microarray data, the study began with 47 231probes, which filtered based on the expression levels from the normalized data. Probes received radiation under 20% was filtered and the study was continued with 47 088 total probe. If any sample received radiation above 20%was allowed to pass through the filter and there by minimize loss of probes. Genes with a standard deviation greater than 0.1 were removed from further analysis. Finally, from the total 47 088 probes 47 071 probes were filtered, and the study were continued with this number of probes [27].

At 60 hours after exposure to 16 Gy of $\gamma^{-60}Co$ radiation in C-4 I cells, the microarray showed that, 105 of the probes expression increased according to the control group (had 2-fold up regulation), and 210 probes expression was lower than the control group (had 2-fold down regulation) (Table 1). In particular, ITPR1 and KREMEN2 had significant up regulation, whereas expressions of MAPK3, MKNK2, SNF and CAP2P were down regulated.

Cellular response to $\gamma^{-60}Co$ radiation is mediated via genes that control complex regulatory pathways such as cell cycle progression, apoptosis, or DNA repair. The relative contribution of changes in the expression of these genes on signaling pathways is unknown [28].

In this study ITPR1, KREMEN2 gene members expression triggers the death of C-4 I cells by WNT and PDGF signaling pathways in $\gamma^{-60}Co$ radiation treated C-4 I cells compared to control cells. The type 1 inositol-1,4,5-trisphosphate receptor (ITPR1) mediates calcium release from the endoplasmic reticulum (ER). ITPR1receptor located on the ER membrane that is critical to calcium homeostasis, was reported to be cleaved during apoptosis in Jurkat cells [29].

Mapk3, Mknk2, Snf ve *Cap2p* gene members of the cell Glycolysis,TGF-β, WNT, PDGF, P38 MAPK, Oxidative stress response andP53signaling pathwayswere significantly down-regulated in $\gamma^{-60}Co$ radiation treated C-4 I compared to control C-4 I cells.

MAPK3 regulates various cellular processes such as proliferation, differentiation, and cell cycle progression in response to a variety of extracellular signals [30]. ERK-1 MAP kinase prevents TNF-induced apoptosis through bad

Table 1: Differentially expressed genes in 16 Gy C-4 I compared to C-4 I control groups from microarray data analysis.

Down-regulated and Up- regulated Genes

Gene Symbol	FC	Expression Changed	Gene Symbol	FC	Expression Changed	Gene Symbol	FC	Expression Changed
LOC644237	-3.79265	down	TIMM17B	-2.15878	down	TNFRSF12A	2.291376	up
MKNK2	-2.14563	down	MTP18	-2.39648	down	TFRC	2.985572	up
MYO18A	-2.62235	down	FAM39E	-2.65507	down	MKI67IP	2.240789	up
NUCB1	-2.21584	down	CLDND2	-2.05717	down	CD44	2.1528	up
MATK	-2.79759	down	ADSSL1	-3.36535	down	EFNB2	2.45524	up
TMEM137	-2.01238	down	HIPK2	-2.82681	down	NOC3L	2.085643	up
SUMF2	-2.38058	down	RNASET2	-2.4344	down	C14orf156	2.517158	up
MAP4	-2.01152	down	RAB40C	-2.04054	down	SAFB	2.643532	up
H19	-2.06486	down	LOC440991	-2.34873	down	CPA4	4.110869	up
PALM	-3.804	down	TMEM44	-2.15751	down	DHRS2	2.033563	up
SLC5A3	-2.52052	down	ASS1	-2.35047	down	ID3	2.00655	up
DUSP3	-2.76101	down	KLK1	-4.50831	down	CYP26B1	2.127379	up
CFD	-2.4075	down	C21orf2	-2.21645	down	SNORD99	2.08307	up
BNIP3L	-2.49273	down	ACSF2	-2.68944	down	ID2	2.360643	up
XYLT2	-2.119	down	YIF1B	-3.10022	down	LOC728216	2.060811	up
ZBTB8A	-2.3723	down	NDUFS8	-2.1055	down	BAZ1A	2.002185	up
PFKL	-2.05159	down	DGCR6	-2.00791	down	TSEN2	2.141856	up
ANKRD9	-3.9042	down	LOC100132535	-2.15071	down	SERPINE2	2.190654	up
GCGR	-2.37948	down	FTHL2	-2.27598	down	RNU6-15	8.252	up
AFAP1	-2.23707	down	WDR54	-3.34919	down	RNU1G2	2.35375	up
LOC644774	-3.31967	down	BCKDHA	-3.36516	down	AADACL4	2.169888	up
WISP2	-2.17586	down	PEMT	-2.08253	down	BDNF	2.537899	up
CARHSP1	-2.25964	down	CSPG4	-3.14984	down	LOC646723	2.195141	up
ENO3	-2.02709	down	SIPA1	-2.37067	down	PSMG1	2.061627	up
SEC63	-3.61088	down	ACSS2	-2.64571	down	CYR61	2.33645	up
LANCL1	-2.14529	down	LOC402538	-2.1107	down	ZMPSTE24	2.423028	up
SFMBT2	-2.79924	down	LUC7L	-2.55621	down	DKK1	3.761853	up
FTHL11	-2.51301	down	ERCC1	-2.04642	down	CTGF	2.747642	up
BNIP3	-4.01959	down	NGFRAP1	-2.30981	down	MSX1	2.368488	up
C17orf61	-2.00805	down	FAM13A	-2.17434	down	NSUN2	2.378491	up
RNU11	-2.94907	down	LOC100132532	-2.47989	down	ITPR1	2.462272	up
GAPDHL6	-2.72929	down	SLC25A23	-2.54784	down	LOC642393	3.323373	up
NDRG1	-4.52317	down	FAM158A	-2.0648	down	RN5S9	17.56618	up
ARL2	-3.57898	down	IDH2	-3.19883	down	HSPH1	2.142729	up
TAF13	-2.27729	down	SLC35C2	-2.34899	down	LOC100132564	3.166493	up
TAF13	-2.36237	down	RPN2	-2.01864	down	RNU6-1	9.159763	up
HMGCS1	-2.31274	down	MIR1974	-3.90058	down	CSTF3	2.687383	up
MAPK3	-2.57397	down	TCEA2	-2.12453	down	SNORD3D	23.12603	up
IL32	-2.29642	down	SYMPK	-2.33338	down	RNU1F1	3.338085	up
RAB13	-4.23306	down	C2orf82	-2.05978	down	ANKRD11	2.237232	up
FOXO4	-2.42097	down	CNNM3	-2.48002	down	RNU1-3	2.226817	up
NFIC	-3.84379	down	ISYNA1	-2.09615	down	CTGF	4.035205	up
RNF165	-2.60303	down	LOC100132288	-3.09848	down	LOC644743	2.194752	up
LOC729992	-2.01011	down	MLXIPL	-2.6806	down	ZNF622	2.11719	up

ALDH3B1	-2.10165	down	ALDH3A1	-2.33893	down	LOC85389	5.139087	up
DCXR	-2.19327	down	C1QTNF6	-2.33846	down	KRT13	2.030385	up
TIAF1	-2.33313	down	NR2F1	-2.98172	down	TIMM10	2.325743	up
LOC387825	-2.03243	down	RAD21	-2.36823	down	SOX17	2.142273	up
FTHL3	-2.51123	down	LRP5	-2.18961	down	LOC100008589	2.830091	up
SPC24	-2.04308	down	NUCKS1	-2.02288	down	LOC100008589	4.945028	up
SLC29A4	-2.58916	down	NR1H3	-2.3109	down	DIO2	2.201815	up
DRD4	-4.1909	down	TMEM91	-2.34252	down	FBN2	4.018469	up
TMEM45A	-2.47835	down	PICK1	-3.41846	down	RNU1A3	3.809543	up
LOC732165	-2.00188	down	BACE2	-2.00435	down	SNORD83B	4.58666	up
HOXA11AS	-2.33246	down	VEGFB	-3.33903	down	COL4A5	2.161077	up
FTH1	-2.28801	down	PPFIA4	-2.43137	down	LOC100132394	7.930195	up
HPCAL1	-2.05276	down	6-Mar	-2.20292	down	C20orf24	2.21874	up
P4HTM	-2.08118	down	CDCP1	-2.21917	down	GNG11	2.536727	up
SEMA3B	-2.01048	down	LOC100129681	-2.23543	down	HNRPM	2.27823	up
SIL1	-2.7212	down	GAPDH	-3.72725	down	LOC644033	2.345024	up
MT1X	-3.91236	down	GAPDH	-2.5513	down	KREMEN2	2.07181	up
LOC729708	-2.26521	down	GAPDH	-2.83752	down	ODC1	2.658591	up
MTE	-2.2616	down	LOC255783	-2.31377	down	UCN2	3.664276	up
CNFN	-2.64449	down	LOC729009	-2.09227	down	MED10	2.382768	up
C17orf49	-2.19878	down	CA9	-4.97239	down	FOXC1	3.688892	up
ACSS2	-2.5716	down	DPP7	-2.09268	down	C20orf199	2.19874	up
ABCB7	-2.31913	down	MC1R	-2.08083	down	KIAA1666	5.516031	up
WSB1	-2.33728	down	LOC391075	-3.35654	down	RNU4-2	3.666893	up
WSB1	-4.53343	down	TOM1	-2.24006	down	RNU1-5	2.101672	up
LOC286016	-2.56499	down	ANGPTL4	-3.56429	down	DCBLD2	2.124149	up
LCAT	-2.59441	down	HOXC4	-2.70585	down	COL7A1	2.209354	up
MT2A	-3.52737	down	PLEKHN1	-2.43137	down	LOC100008588	2.152983	up
UBXN6	-2.46764	down	TMUB1	-2.3716	down	C20orf24	2.253316	up
ENO2	-4.53821	down	SEZ6L2	-2.23582	down	LOC100134364	2.357778	up
NUCKS1	-2.33179	down	PRNPIP	-2.54991	down	ALB	3.306516	up
C21orf58	-2.12242	down	ANKRD33	-2.16356	down	LOC652235	2.040471	up
RAB4B	-2.15139	down	ZNF526	-2.58858	down	SNORD10	4.737826	up
SFN	-2.2933	down	WFDC1	-2.05472	down	SLC38A2	2.039199	up
ITGA5	-3.35222	down	TRAPPC6A	-2.44657	down	IFIT2	2.073076	up
LOX	-3.4269	down	DGCR6	-2.05774	down	DNMT1	2.022657	up
MT1A	-3.23128	down	HCFC1R1	-3.06927	down	RNU4-1	5.894303	up
LOC401252	-2.46926	down	HCFC1R1	-3.76447	down	SNORD3C	36.81438	up
DSEL	-3.96844	down	PTOV1	-2.09268	down	RNU12	2.183622	up
FSCN2	-2.11908	down	FAM162A	-3.0414	down	IGF2BP3	2.068923	up
ALDOC	-7.30546	down	ALDOA	-2.28242	down	CALD1	2.131286	up
CD68	-2.25926	down	SLC16A3	-2.5165	down	SNORA67	2.211227	up
P2RY11	-2.00458	down	MUC1	-2.29842	down	RPPH1	2.029684	up
DNAJB2	-2.24918	down	RPL14	-3.42951	down	PPAP2B	2.075177	up
LOC100131713	-2.1291	down	PDDC1	-2.07092	down	SNORA73A	2.114524	up
C12orf10	-2.13759	down	TMEM205	-2.01323	down	FAM179A	2.471054	up
LOC388076	-2.05928	down	PDE9A	-2.5926	down	RN7SK	6.741672	up

SLC6A10P	-3.11781	down	PRKCSH	-2.03108	down	RN7SK	10.69681	up
CSNK1E	-2.33995	down	CAPZB	-2.00726	down	ASPM	2.49661	up
VKORC1	-2.82645	down	HOXC10	-2.20101	down	TXNDC14	2.025069	up
BCKDK	-3.0848	down	TLE6	-2.2353	down	ERH	2.325561	up
OPA3	-2.14989	down	C14orf78	-2.0409	down	PTPLAD1	2.064264	up
C12orf11	-2.27695	down	GPI	-2.63082	down	DUSP1	2.493636	up
NDUFA4L2	-3.5262	down	PTP4A2	-2.34826	down	TXNRD1	2.00262	up
SLC2A3	-3.09976	down	PC	-2.14352	down	HINT3	4.739621	up
RRBP1	-2.11126	down	C11orf80	-2.46962	down	LOC642035	4.515363	up
KRT17	-2.21779	down	CDT1	-2.22267	down	ANXA1	2.227672	up
MED16	-2.10614	down	HIST1H1C	-2.5455	down	SNORD3A	26.58271	up
ERI3	-2.78666	down	LHPP	-2.50539	down	SNORD12C	2.324122	up
TMEM219	-2.14872	down	LOC	-2.02106	down	GTPBP4	2.188588	up
Abbreviations: [FC: Fold Change.]								

phosphorylation and inhibition of Bax translocation in HeLa Cells [31].

MKNK2 protein is one of the downstream kinases activated by mitogen-activated protein (MAP) kinases. It playing important roles in the initiation of mRNA translation, oncogenic transformation and malignant cell proliferation [32].

GO and pathways analysis identified the cell glycolysis related pathways were significantly down-regulated in gamma radiation treated C-4 I cells compared to control cells. Several gene members of the cell glycolysis related pathways were significantly down-regulated in gamma radiation treated C-4 I cells compared to control cells. Most cancer cells exhibit increased glycolysis and use this metabolic pathway for generation of ATP as a main source of their energy supply. Thus, combination of glycolytic inhibitors and DNA-damaging agents seems to be an attractive therapeutic strategy to effectively kill cancer cells [33].

Gene expressions by qRT-PCR

To gain insights into radiation response, qRT-PCR was used to assess expression patterns of many apoptosis-related genes, grouped to reflect the various protein families and pathways involved in apoptosis, in C-4 I cells at 60 hours after exposure to 16 Gy single dose of $\gamma^{-60}Co$ radiation (Figure 4).

In this part of the present study, it was hypothesized that apoptosis-related gene expression levels in C-4 I cells were affected by $\gamma^{-60}Co$ radiation. Figure (5) shows that the apoptosis-related genes *Bid, Bik, Pmiip1, Traf2, Traf3, Traf6, Tnf, Tnfrsf10b, Tnfrsf10d, Tp53ı3, Socs2, Socs3, Nf-kb1, Nf-kb2, Cradd, Pten,Dffa, Fam96a* and *Fam96b* were up-regulated (FC ≥2). While other apoptosis-related *Bcl2l2, Bcl2l13, Bag1, Bad, Cad, Hrk, Fadd, Traf7, Tp53, Stat5b* and *Relb* gene expression levels were down-regulated (FC ≥ -2) (Figure 5).

There are two main apoptotic pathways: The extrinsic apoptotic pathway involves engagement of particular death receptors that belong to the TNFR (Tumor Necrosis Factor Receptor) family and, through the formation of the DISC (Death-Inducing-Signaling-Complex), leads to a cascade of activation of Caspases, including Caspase 8 and Caspase 3, which in turn

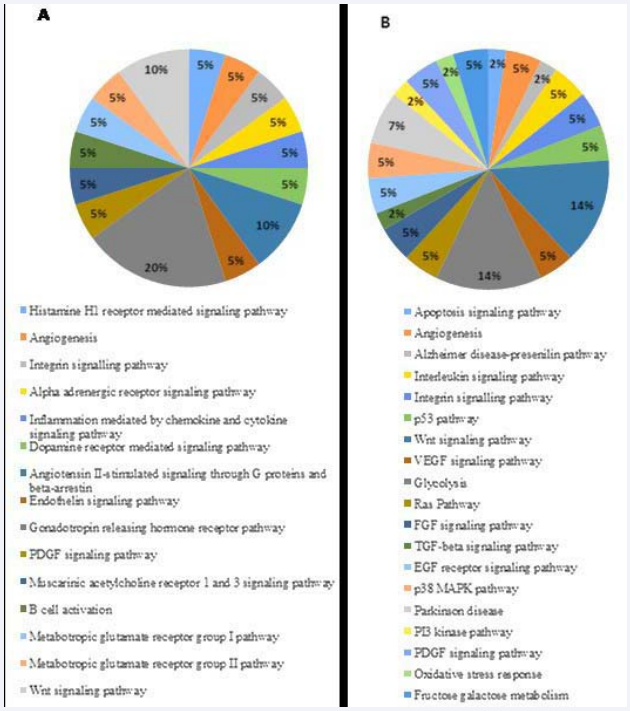

Figure 4 Pie charts showing pathways altered in C-4 I cells at 60 hours after exposure to 16 Gy single dose of gamma radiation, as compared to control cells. Chart was generated from the microarray data analysis according to PANTHER pathway enrichment analysis. (A) were performed on up-regulated genes. (B) Were performed on down-regulated genes.

induce apoptosis. Our results were in agreement with previous results that found the death-domain-containing receptor for TRAIL (TNF-Related Apoptosis-Inducing Ligand) was induced by P53 in response to DNA damage and in turn promotes cell death through Caspase 8. Thus, the extrinsic apoptotic pathway was activated by inducing the expression of TRAIL death receptor in response to $\gamma^{-60}Co$ radiation of C-4 I cells [34,35].

The Intrinsic apoptotic pathway is dominated by the BCL2 family of proteins, which governs the release of Cytochrome-C

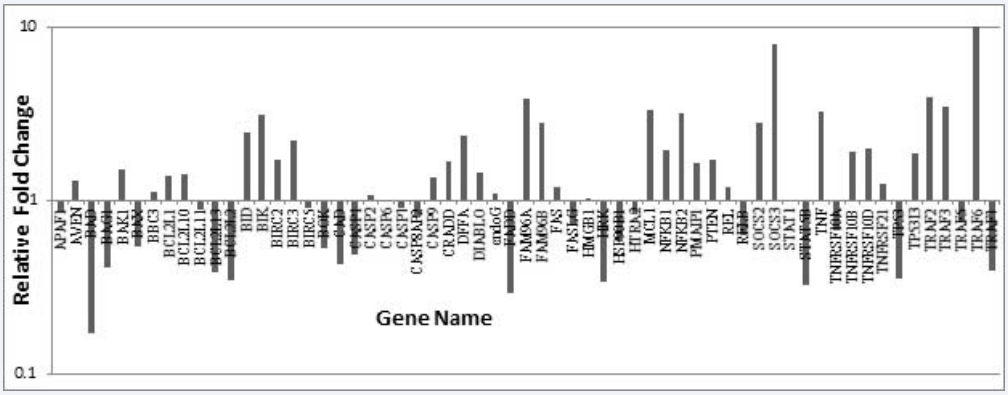

Figure 5 Fold changes of genes involved in apoptosis in C-4 I cells at 60 hours after exposure to 16 Gy single dose of gamma radiation.

(CytoC) from the mitochondria. BCL2 family comprises anti-apoptotic (pro-survival) and pro-apoptotic members. From our results radiation induced a pro-apoptotic BID and BIK genes expression in C-4 I cells. BID, a critical link between the extrinsic apoptosis pathway with the mitochondrial pathway in certain cell types [36]. This gene encodes a death agonist that hetero dimerizes with either agonist BAX or antagonist BCL2. It is a mediator of mitochondrial damage induced by caspase-8 [37,38].

BIK, as a BH-only pro-apoptotic member, binds with BCL-2, BCL2L1 or MCL-1 to replace BAX or BAK, which forms BAX/BAK oligomerization and then triggers mitochondrial outer membrane permeabilization, cytochrome c into cytoplasm, caspase-9 activation and at last cell apoptosis [39]. Hur et al. [40], suggest that expression of BIK in human breast cancer cells is regulated at the mRNA level by a mechanism involving a non transcriptional activity of P53 by gamma radiation and by proteasomal degradation of BIK protein. Jiao et al. [41], generated a novel mutant form of BIK, as a therapeutic gene for breast cancer. Therefore, BIK and its mutant forms can be a novel therapeutic gene in cervix cancer targeted gene therapy.

Our results also suggested that radiation decreased gene expression of the BCL-2 family anti-apoptotic members. In a study conducted by Loriot et al. [42], radiotherapy has a critical role in the treatment of small-cell lung cancer (SCLC). The effectiveness of radiation in SCLC remains limited as resistance results from defects in apoptosis. Their results show the inhibition of BCL-2/BCL-XL can enhance radiosensitivity of SCLC lung cancer cells *in vitro* and *in vivo*.

In another study Wu et al. [43], support the combination of radiation and pro-survival Bcl-2 family inhibitor as a potential novel therapeutic strategy in the local-regional management of breast cancer.

CONCLUSION

This *in vitro* study presents the altering in gene expression and pathway analysis of gamma irradiation in cervical cancer C-4 I cells. This study reveals that gamma radiation induced the pro-apoptosis *Bid, Bik, Traf2, Traf3, Traf6, Tnf, Tnfrsf10b, Tnfrsf10d* and other gene expressions in C-4 I cells presumably and it may be a down-regulator of some anti-apoptotic gene expression levels. These results indicate that single dose of $\gamma^{-60}Co$ irradiation primarily affects C-4 I cells proliferation by inducing the intrinsic and extrinsic apoptotic pathways. Identification of specific genes may allow the determination of pathways important in radiation responses, that it may be beneficial in novel treatment strategy to increase the cancer cell sensitivity to radiotherapy by modulation of many genes expression.

ACKNOWLEDGEMENTS

This study was supported by project number 25190 of the Research Fund at University of İstanbul.

REFERENCES

1. Nair S, Nair RR, Srinivas P, Srinivas G, Pillai MR. Radiosensitizing effects of plumbagin in cervical cancer cells is through modulation of apoptotic pathway. Mol Carcinog. 2008; 47: 22-33.
2. Li B, Zhao J, Wang CZ, Searle J, He TC, Yuan CS, et al. Ginsenoside Rh2 induces apoptosis and paraptosis-like cell death in colorectal cancer cells through activation of p53. Cancer Lett. 2011; 301: 185-192.
3. Bhosle SM, Huilgol NG, Mishra KP. Apoptotic index as predictive marker for radiosensitivity of cervical carcinoma: Evaluation of membrane fluidity, biochemical parameters and apoptosis after the first dose of fractionated radiotherapy to patients. Cancer Detection and Prevention. 2005; 29: 369-375.
4. Wyllie AH. "Where, O death, is thy sting?" A brief review of apoptosis biology. Mol Neurobiol. 2010; 42: 4-9.
5. John H, Maduro MD, Elisabeth GE, De Vries MD, Gert-Jan M, Brigitt, MT, et al. Targeting Pro- Apoptotic TRAIL Receptors Sensitizes HeLa Cervical Cancer Cells to Irradiation-Induced Apoptosis. Int J Radiat Oncol Biol Phys. 2008; 72: 543-552.
6. Eriksson D, Löfroth PO, Johansson L, Riklund K, Stigbrand T. Apoptotic signalling in HeLa Hep2 cells following 5 Gy of cobalt-60 gamma radiation. Anticancer Res. 2009; 29: 4361-4366.
7. Frenzel A, Grespi F, Chmelewskij W, Villunger A. Bcl2 family proteins in carcinogenesis and the treatment of cancer. Apoptosis. 2009; 14: 584-596.
8. Jiang B, Liang P, Deng G, Tu Z, Liu M, Xiao X. Increased stability of Bcl-2 in HSP70-mediated protection against apoptosis induced by oxidative stress. Cell Stress Chaperones. 2010; 16:143-152.
9. Inoue S, Browne G, Melino G, Cohen GM. Ordering of caspases in cells undergoing apoptosis by the intrinsic pathway. Cell Death Differ. 2009; 16: 1053-1061.
10. Zhou Y, Feng X, Koh DW. Activation of Cell Death Mediated by Apoptosis-Inducing Factor Due to the Absence of Poly(ADP-ribose) Glycohydrolase. Biochemistry. 2011; 50: 2850-2859.

11. Cui Q, Yu JH, Wu JN, Tashiro S, Onodera S, Minami M, et al. P53-mediated cell cycle arrest and apoptosis through a caspase-3-independent, but caspase-9-dependent pathway in oridonin-treated MCF-7 human brea... Acta Pharmacol Sin. 2007; 28: 1057-1066.

12. Bian J, Wang X, Yun J, Cao R, Cao Y, Liang J, et al. Single-fraction γ-60Co radiation induces apoptosis in cultured rat C6 cells. Ann Saudi Med. 2012; 32: 269-275.

13. Arican GO, Khalilia W, Serbes U, Akman G, Cetin I, Arican E. Effects of hypobaric conditions on apoptosis signalling pathways in HeLa cells. APJCP. 2014; 15; 5043-5047.

14. Banáth JP, Macphail SH, Olive PL. Radiation sensitivity, H2AX phosphorylation, and kinetics of repair of DNA strand breaks in irradiated cervical cancer cell lines. Cancer Res. 2004; 64: 7144-7149.

15. Smirnov DA, Brady L, Halasa K, Morley M, Solomon S, Cheung VG. Genetic variation in radiation-induced cell death. Genome Res. 2012; 22: 332-339.

16. zcan Arican G, akir , Arican E, Turgut Kara N, Dagdeviren , Ari S. Effects of Geven root extract on proliferation of HeLa cells and bcl-2 gene expressions, African Journal of Biotechnology. 2012; 11: 4296-4304.

17. Gieseler RK, Marquitan G, Schlatt JM, Sowa L P, Bechmann J, Timm M, et al. Hepatocyte apoptotic bodies encasing nonstructural HCV proteins amplify hepatic stellate cell activation: implications for chronic hepatitis C. J Viral Hepat. 2011; 18: 760-767.

18. Hrvatin S, O'Donnell CW, Deng F, Millman JR, Pagliuca FW, DiIorio P, et al. Differentiated human stem cells resemble fetal, not adult, β cells. Proc Natl Acad Sci U S A. 2014; 111: 3038-3043.

19. Pera J, Korostynski M, Krzyszkowski T, Czopek J, Slowik A, Dziedzic T, et al. Gene expression profiles in human ruptured and unruptured intracranial aneurysms: what is the role of inflammation? Stroke. 2010; 41: 224-231.

20. Reinholz MM, Eckel-Passow JE, Anderson SK, Asmann YW, Zschunke MA, Oberg AL, et al. Expression profiling of formalin-fixed paraffin-embedded primary breast tumors using cancer-specific and whole genome gene panels on the DASL platform. BMC Medical Genomics. 2010; 3: 60.

21. Mi H and Thomas P. PANTHER Pathway: An Ontology-Based Pathway Database Coupled with Data Analysis Tools. Methods Mol Biol. 2009; 123-140.

22. Wilkie GS, Gautier P, Lawson D, Gray NK. Embryonic Poly(A)-Binding Protein Stimulates Translation in Germ Cells. Mol Cellular Biol. 2005; 25: 2060-2071.

23. Willems E, Leyns L, Vandesompele J. Standardization of real-time PCR gene expression data from independent biological replicates. Anal Biochem. 2008; 379: 127-129.

24. Hellemans J, Mortier G, De Paepe A, Speleman F, Vandesompele J. qBase relative quantification framework and software for management and automated analysis of real-time quantitative PCR data. Genome Biol. 2007; 8: R19.

25. Liu SS, Chan KY, Leung RC, Law HK, Leung TW, Ngan HY. Enhancement of the radiosensitivity of cervical cancer cells by overexpressing p73alpha. Mol Cancer Ther. 2006; 5: 1209-1215.

26. Maduro JH, de Vries EGE, Meersma GJ, Hougardy BMT, van der Zee AGJ, de Jong S. Targeting Pro-Apoptotic TRAIL Receptors Sensitizes HeLa Cervical Cancer Cells to Irradiation-Induced Apoptosis. IJR OBP. 2008; 72: 543-552.

27. Feng J, Sheng H, Zhu C, Jiang H, Ma S. Effect of Adjuvant Magnetic Fields in Radiotherapy on Non-Small-Cell Lung Cancer Cells In Vitro. BioMed Res Int. 2013; e657259.

28. Chaudhry MA. Analysis of gene expression in normal and cancer cells exposed to gamma-radiation. J Biomed Biotechnol. 2008; 541678.

29. Elkoreh G, Blais V, Béliveau E, Guillemette G, Denault JB. Type 1 inositol-,4,5-trisphosphate receptor is a late substrate of caspases during apoptosis. J Cell Biochem. 2012; 113: 2775-2284.

30. Liu F, Zheng S, Liu T, Liu Q, Liang M, Li X. et al. MicroRNA-21 promotes the proliferation and inhibits apoptosis in Eca109 via activating ERK1/2/MAPK pathway. Molecu Cellul Biochem. 2013; 381: 115-125.

31. Pucci B, Indelicato M, Paradisi V, Reali V, Pellegrini L, Aventaggiato M, et al. ERK-1 MAP kinase prevents TNF-induced apoptosis through bad phosphorylation and inhibition of Bax translocation in HeLa Cells. J Cell Biochem. 2009; 108: 1166-1174.

32. Buxade M, Parra-Palau JL, Proud CG. The Mnks: MAP kinase-interacting kinases (MAP kinase signal-integrating kinases). Front Biosci. 2008; 13: 5359-5373.

33. Pelicano H, Martin DS, Xu RH, Huang P. Glycolysis inhibition for anticancer treatment. Oncogene. 2006; 25: 4633-4646.

34. Kim S, Zhang L. Identification of naturally secreted soluble form of TL1A, a TNF-like cytokine. J Immunol Methods. 2005; 298: 1-8.

35. Ihrie RA, Bronson RT, Attardi LD. Adult mice lacking the p53/p63 target gene Perp are not predisposed to spontaneous tumorigenesis but display features of ectodermal dysplasia syndr... Cell Death Differ. 2006; 13: 1614-1618.

36. Wang P, Lindsay J, Owens TW, Mularczyk EJ, Warwood S, Foster F, et al. Phosphorylation of the proapoptotic BH3-only protein bid primes mitochondria for apoptosis during mitotic arrest. Cell Rep. 2014; 7: 661-671.

37. Garcia-Perez C, Roy SS, Naghdi S, Lin X, Davies E, Hajnczky G. BID-induced mitochondrial membrane permeabilization waves propagated by local reactive oxygen species (ROS) signaling. Proceedings of the National Academy of Sciences of the United States of America. 2012; 109: 4497-4502.

38. Wang Y, Tjandra N. Structural insights of tBid, the caspase-8-activated Bid, and its BH3 domain. J Biol Chem. 2013; 288: 35840-35851.

39. Certo M, Del Gaizo, Moore V, Nishino M, Wei G, Korsmeyer S, Armstrong SA, et al. Mitochondria primed by death signals determine cellular addiction to antiapoptotic BCL-2 family members. Cancer Cell. 2006; 9: 351-365.

40. Hur J, Bell DW, Dean KL, Coser KR, Hilario PC, Okimoto RA, et al. Regulation of expression of BIK proapoptotic protein in human breast cancer cells: p53-dependent induction of BIK mRNA by fulvestrant and proteasomal degradation of BIK protein. Cancer Res. 2006; 66: 10153-10161.

41. Jiao S, Wu M, Ye F3, Tang H, Xie X, Xie X. BikDDA, a mutant of Bik with longer half-life expression protein, can be a novel therapeutic gene for triple-negative breast cancer. PLoS One. 2014; 9: 92172.

42. Loriot Y, Mordant P, Dugue D Geneste O, Gombos A, Opolon P, et al. Radiosensitization by a novel Bcl-2 and Bcl-XL inhibitor S44563 in small-cell lung cancer. Cell Death Dis. 2014; 5: e1423.

43. Wu H, Schiff DS, Lin Y, Neboori HJ, Goyal S, Feng Z, et al. Ionizing radiation sensitizes breast cancer cells to Bcl-2 inhibitor, ABT-737, through regulating Mcl-1. Radiat Res. 2014; 182: 618-625.

Cite this article

Khalilia WM, Özcan G, Karaçam S (2017) Gene Expression and Pathway Analysis of Radiation-Induced Apoptosis in C-4 I Cervical Cancer Cells. J Autoimmun Res 4(1): 1014.